



OPEN ACCESS

EDITED BY

Jacob B. Lowenstern,
United States Geological Survey (USGS),
United States

REVIEWED BY

Simon Thivet,
UMR6524 Laboratoire Magmas et
Volcans (LMV), France
Natalia Gauer Pasqualon,
University of Hawaii at Manoa,
United States

*CORRESPONDENCE

Dork Sahagian,
✉ dos204@lehigh.edu

RECEIVED 10 March 2023

ACCEPTED 21 April 2023

PUBLISHED 09 May 2023

CITATION

Moyer S and Sahagian D (2023), Cry me a
Pele's tear: new insights on the internal
structures of Pele's tears.
Front. Earth Sci. 11:1184027.
doi: 10.3389/feart.2023.1184027

COPYRIGHT

© 2023 Moyer and Sahagian. This is an
open-access article distributed under the
terms of the [Creative Commons
Attribution License \(CC BY\)](#). The use,
distribution or reproduction in other
forums is permitted, provided the original
author(s) and the copyright owner(s) are
credited and that the original publication
in this journal is cited, in accordance with
accepted academic practice. No use,
distribution or reproduction is permitted
which does not comply with these terms.

Cry me a Pele's tear: new insights on the internal structures of Pele's tears

Scott Moyer and Dork Sahagian*

Lehigh University, Bethlehem, PA, United States

In this paper we present novel observations of internal structures of Pele's tears and spheres revealed from SEM studies of particles formed within Kilauean lava fountains. Partially weathered Pele's tears from eruption episodes in 1969 include a crust, or rind, of material that is smooth on the external surface. However, once this crust is peeled away, it reveals a sub-crustal surface within the tear that is morphologically complex. This surface is characterized by a network of ridges and valleys that warp around radial structures with pores at their centers. The ridges and valleys are interpreted to represent the differential cooling and shrinkage of the external surface of the spheres and tears relative to the interior upon exiting the lava fountain and chilling in ambient air. The radial structures are interpreted to be formed as result of chemical zonation within the cooling at locations where a vesicle contacts the external crust. An additional feature is observed on the underside of crust that is peeled off each tear. This surface has a roughly polygonal network of tubes that surround pores at the center of many of the polygons. The tubes are hollow and some contain solid material within, possibly the remains of the crushed top of the tube where the SEM can peer inside. The origin of this tube network is a puzzle remaining to be solved.

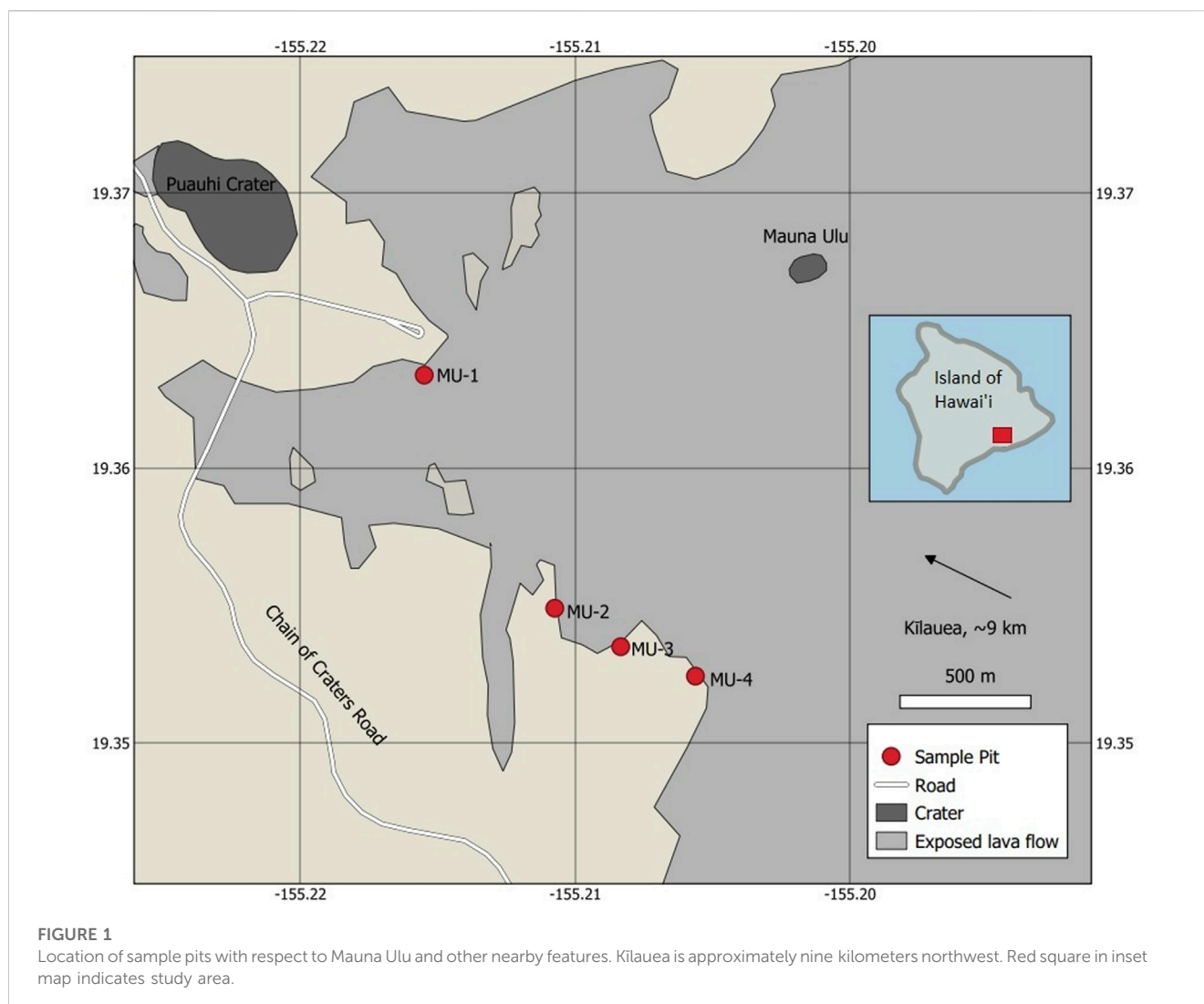
KEYWORDS

Pele's tears, Pele's spheres, lava fountains, Hawaii eruptions, Kilauea (Hawaii), spherulites

Introduction

Pele's tears are common pyroclasts produced during Hawaiian-type volcanic eruptions in the form of lava fountains, and their morphology can provide insights regarding eruptive processes (Moune et al., 2007; Porritt et al., 2012; Wygel et al., 2019). Lava fountains are produced by the rapid exsolution and expansion of H₂O bubbles from a melt (Gerlach, 1986; Head & Wilson, 1987; Wilson et al., 1995). After fragmentation of a magmatic foam in a lava fountain, continued exsolution of H₂O and other oversaturated volatiles produces additional bubbles within Pele's tears after these droplets have formed (Proussevitch & Sahagian, 1996; Porritt et al., 2012; Thivet et al., 2020). Tears and spheres form from fragments of bubble walls and Plateau borders during viscous relaxation due to surface tension before quenching. In extreme cases of shear strain prior to solidification, fragments may stretch to become Pele's hair (Moune et al., 2007).

While adiabatic cooling of gas bubbles within Pele's tears may assist in cooling the outer portions of the tear below the glass transition temperature (Namiki et al., 2021), Pele's tears can only be preserved intact when the center of the tear is fully cooled below the glass transition temperature before gas bubbles inside can expand to the point of fracturing the tear (Porritt et al., 2012). However, post-fragmentation evolution and deformation is still



observed in tears as well as in larger pyroclasts (Browning et al., 2020; Tuffen et al., 2022) and breadcrust bubbles (Quane and Andrews, 2020).

Previous work regarding the interior of Pele's tears (Porritt et al., 2012) and hair (Cannata et al., 2019) from Hawaiian volcanoes focused on bubble vesicle properties and distributions. In an exploratory investigation of lava fountaining and Pele's tear vesicularity, we examined material collected in the proximity of Mauna Ulu, approximately nine kilometers southeast of the main Kilauea caldera in Hawai'i. Unexpected structures were observed beneath the glassy surface rind of the tears, positioned among an interior matrix of complex textures not previously described in detail. In addition, a perplexing network of tubes has been observed on the underside of the glassy rind. These textures may provide insights regarding the processes that occur within lava fountains and related effusive eruptions of basaltic volcanoes.

A potential interpretation of some of the structures observed beneath the surface of Pele's tears is that they are spherulitic textures created by radial crystal growth as a result of chemical zonation during the cooling of the tears. Previously observed examples of spherulites in Hawaiian basalts have been dendritic overgrowths on

plagioclase crystals from Makaopuhi crater (Lofgren, 1971a). Spherulites are most common in Archaean basalts, but are found in modern examples as well (Fowler et al., 2002). Spherulitic textures consisting of quartz, clinopyroxene, or feldspar crystals radiating outward from a central point or pore space have been observed in a variety of glassy or microcrystalline volcanic rocks (Chisholm, 1911; Lofgren, 1971a; Shtukenberg et al., 2012). Spherulite crystal growth is initiated due to a low temperature impurity at the interface of the growing crystal phase (Lofgren, 1971a) and is indicative of rapid crystallization (Dietrich & Skinner, 1979) due to undercooling of the melt (Kirkpatrick et al., 1979), as would have been the case of Pele's tears in a lava fountain.

To test the hypothesis that the structures observed in Pele's tears are spherulites, point chemical analysis was performed to determine if there is a significant difference in the chemical compositions of the radial textures and the surrounding matrix material. A significant difference would support a spherulitic mechanism, noteworthy because previous descriptions of spherulitic textures have been at a scale of millimeters or greater (Smith et al., 2001; Fowler et al., 2002; Shtukenberg et al., 2012) as opposed to the μm scale observed in Pele's tears and spheres.

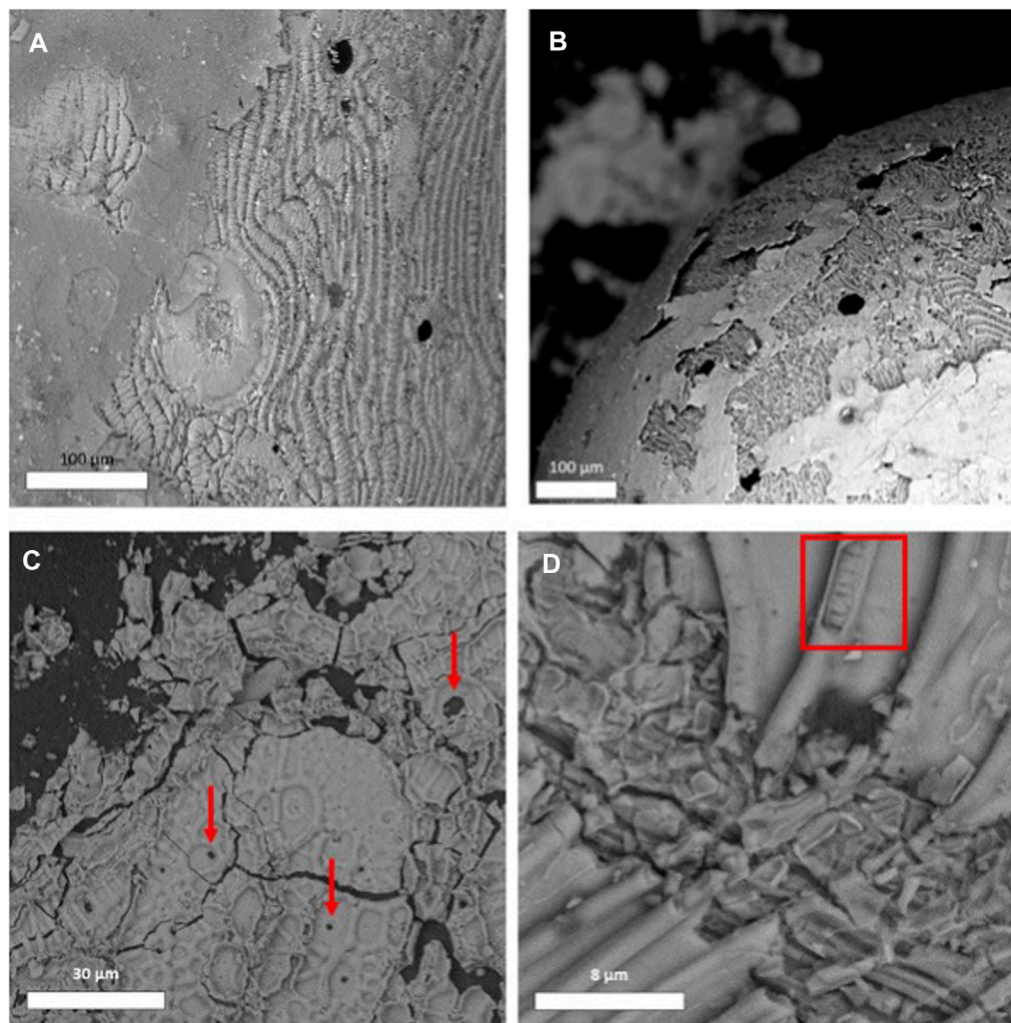


FIGURE 2

Top: Examples of the radial structures visible when the exterior crust of the tears peeled away. The images in (A, B) clearly show the crust peeling away, confirming that these radial structures are a feature which sits within the tear itself and not a texture which has developed or grown on the exterior of the tear. They sit in a matrix which displays a texture similar to corn on the cob (left) or ridges and valleys (right). Bottom: Examples of the branching networks of tubes observed on the undersides of the glassy crust of the tears. These tears were sampled from the uppermost eight centimeters of sample pits MU-3 and MU-4. The red arrows in (C) point to some pores that fully penetrate the glassy crust. The red rectangle in (D) highlights an area where the interior of a tube is visible.

Methods

The tears examined for the present study were collected from permitted sample pits approximately nine kilometers southeast of Kilauea in Hawai'i Volcanoes National Park, in coordination with the Hawaiian Volcano Observatory (Figure 1). The collected pyroclasts come from deposits associated with the 1969 eruption of Mauna Ulu. This eruption began in May 1969 and lasted until December 1971, but the main lava fountaining episodes occurred during the first phase of the eruption from May to December 1969 (Swanson et al., 1979; Parcheta et al., 2012; Parcheta et al., 2013). The majority of the tears in question were collected from the upper 8 centimeters of their respective sample pits, with a few exceptions. Consequently, their exteriors are weathered to varying degrees and are stained orange by oxidation in some patches, potentially from leached iron and other metals (Wygel et al., 2019). The sample pits

are designated as MU-2, MU-3, and MU-4. Pele's tears were collected from a depth of 7–8 centimeters from Pit MU-2, from 6 to 8 centimeters from Pit MU-3, and from 0 to 2 centimeters from Pit MU-4. Based on ashfall maps of the 1969 eruption published by Parcheta et al. (2013), these tears were produced during lava fountaining episodes 10, 11, and 12 of the 1969 eruption.

Eleven examples of Pele's tears were examined under a Phenom-XL scanning electron microscope (SEM). The length of the long axis of tears ranged from one to three mm with a maximum aspects ratio of 2:1. During initial mounting of the tears, they were rolled on the sticky pad of the SEM stub so that the glassy crust of the tears might be peeled away. A series of images was obtained at varying levels of magnification, so that detailed pictures of individual features could be acquired along with their relative positions. Chemical analysis using energy dispersive X-ray analysis (EDX) provided general comparisons between the observed structures and the

background materials. A series of points were examined in the matrix material, on the radial structures, and on the top and underside of the glassy crust. Sample size was 24 points for the matrix material and 20 points for the radial structures. Chemical composition was interpreted using the Phenom Pro Suite software available with the SEM.

Additional physical and chemical examinations were carried out on a Zeiss EVO-25 scanning electron microscope. These were completed after the samples of Pele's tears were coated in gold to increase conductivity and reflectivity. Gold was consequently disabled in the element identification software of the SEM. No artifacts due to the coating were observed, and while the weight percent compositions found using this machine are somewhat altered due to the overprinting of gold, the relative ratios of elements present in the tears should remain accurate.

Results

Textural analysis

Viewed under the SEM, it could be seen that portions of the glassy crust of one of the tears has peeled away, revealing structures beneath the surface (Figure 2). These structures are generally radial features centered around a core divot or pore. The size and elongation varies with each feature. The smallest are on the order of 20 μm in diameter and are generally circular. The largest radial structure to be measured has a long-axis diameter of 154 μm .

Separating the radial features is a matrix which displays small ridges and valleys, arranged in varying geometries. In some areas the ridges form parallel segments, while in others they take on a mud-cracked or scaly texture. The individual ridges are generally a single μm wide and separated by a valley about 5 μm across. In areas where vesicles intersect the surface of the tear, it appears that the ridge features are warped around the vesicle itself, so that ridges and valleys did not intersect the vesicle. Ridges also warp around radial structures, suggesting either that the ridges post-date the structures, or that they were sufficiently fluid at the time the structures developed to deform. Subsequent examinations of several more tears revealed similar features, although two of these tears are severely weathered and the structures are poorly preserved. In place of the ridge and valley texture observed in the initial tear, some of these other tears showed portions of matrix texture similar to corn on the cob (Figure 2).

Portions of the glassy crust which had been stuck to the SEM stub were exposed such that their undersides could be examined. Interestingly, these crusts have a branching network of tubes along their undersides (Figure 2). From images obtained on the SEM, the interior diameter of the largest of these tubes is estimated to be 3.5 μm . In some places where the tubes have cracked open, solidified material could be seen inside. This material resembles a single row of the corn-cob-textured matrix seen elsewhere in the tear. In other areas where the interiors of the tubes were exposed the tubes just contain empty space. The interior diameter of the cracked tubes is generally 2 μm across. Where pores penetrate all the way through the glassy crust, the network of tubes circumvents these areas and avoids contact with the pores. The network appears to branch in two dimensions only, with no obvious tubes facing up towards the

receiver (corresponding with a tube penetrating deeper into the tear).

Chemical analysis

Point analysis of chemical composition using EDX shows considerable variation between the different regions observed. An unpaired *t*-test indicates that there are significantly different weight concentrations of iron and silicon in the matrix material compared to the radial structures. The *p*-value is 0.0072 for both iron and silicon, indicating the values are significantly different.

The average weight concentration of iron is 19.33% in the matrix and 12.24% in the radial structures, while the average weight concentration of silicon is 18.43% in the matrix and 21.18% in the radial structures. Plotting the iron composition as a function of silicon content, there is a strong negative correlation in matrix material ($R^2 = 0.71$), while iron content is constant and independent of silicon in the radial structures (Figure 3).

Additional element mapping performed with the Phenom-XL SEM and chemical profile analysis performed on the Zeiss EVO-25 SEM generally confirmed these findings (Figure 4). Analysis of several linear profiles along the surface indicated for the most part that silicon content increases as the profile passes over portions of the radial structures.

Discussion

The morphology and chemical distribution of the radial structures suggests a spherulitic texture caused by radial growth of clinopyroxene and/or plagioclase feldspar crystals following sub-surface chemical zonation (Chisholm, 1911; Lofgren, 1971a; Shtukenberg et al., 2012). It is unlikely that differential cooling or melt flooding of near-surface vesicles caused the observed textures. The observed structures are similar to spherulites in that generally they appear to be made of thin crystals radiating outward from a central cavity (Chisholm, 1911; Lofgren, 1971a; Shtukenberg et al., 2012). If the inverse were true and molten material was penetrating a vesicle before solidifying, there would probably not be such a consistent pattern of crystal growth (Phillips, 1973). Spherulites can also be produced by the devitrification of glass as it continues to cool below its glass transition temperature (Lofgren, 1971b). When this is the case there are often cracks associated with the spherulites (Monecke et al., 2003). Since there are no obvious cracks associated with the spherulites observed in these samples of Pele's tears, it follows that the spherulites formed from the primary melt rather than devitrification of the glass. Additionally, no spherulites have been observed in the glassy outer crust of Pele's tears but instead appear just below the surface. Devitrification of the glass would likely affect all layers of the tears. Further, examination of Pele's hair indicated no evidence of spherulites or valley-ridge textures beneath portions of peeled crust. Had devitrification been the mechanism for formation of spherulites found in tears, it would have also occurred in Pele's hair. We interpret the apparent absence of these textures in Pele's hair to be due to the extreme shear strains involved that would have stretched out any textures to beyond recognizability.

The branching network of tubes on the underside of the crustal material and radial structures between valley-ridge morphology

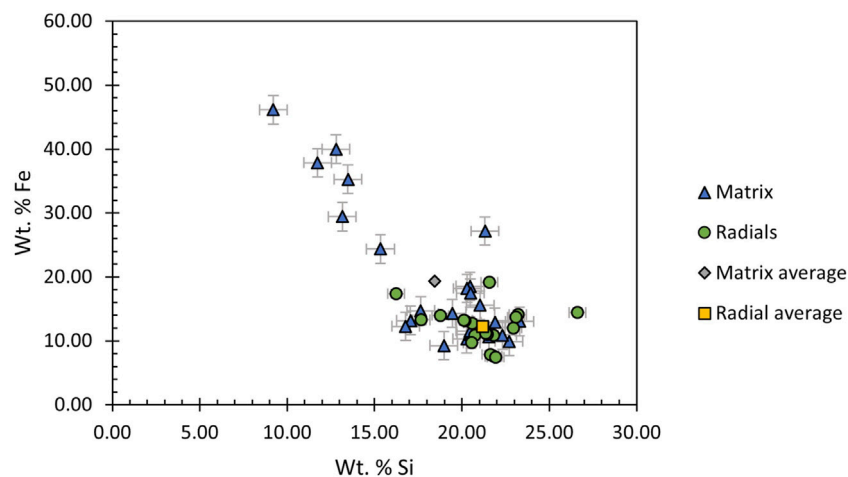


FIGURE 3

Concentrations (wt%) of iron plotted against concentrations of silicon for each point analyzed on Pele's tears from Mauna Ulu. There is an obvious negative correlation between iron and silicon in the case of the matrix material ($R^2 = 0.71$), but this same correlation is not evident among the points examined in the radial structures. A value of nearly 50% Fe suggests the presence of micro-crystalline magnetite or other iron oxides that dilute Si in the matrix but not in the radial structures that show greater variability in Si than Fe.

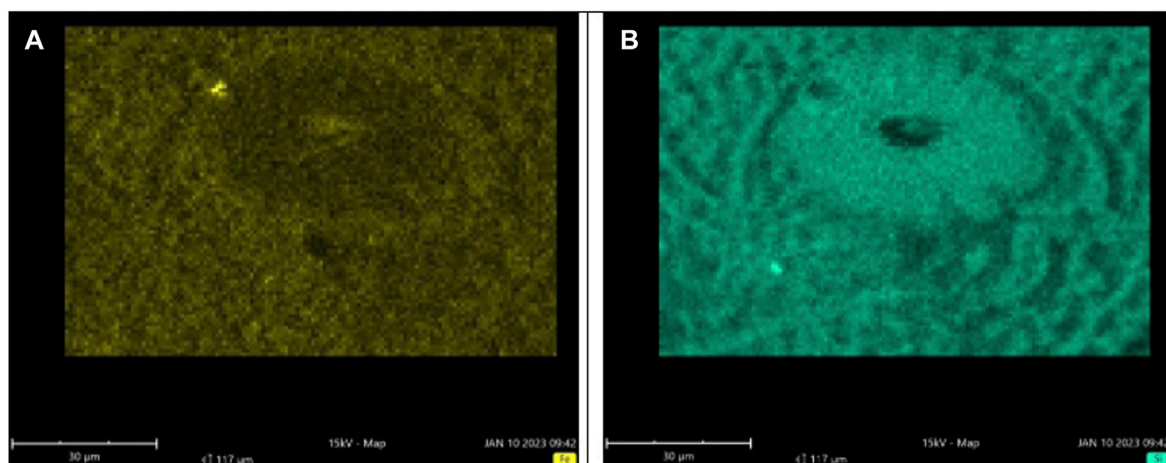


FIGURE 4

(A) Map of iron content through a radial structure, with a notable donut-shaped void where the structure itself sits. (B) Map of silicon content around that same radial structure, showing consistently higher concentrations in the structure. Surface topography may affect apparent concentrations outside the radial structure, but the relative concentrations of Fe vs. Si are not influenced.

observed in the matrix material are probably made by different mechanisms. Voids can be created in larger pyroclasts like lava bombs due to tensile forces produced by uneven cooling over time (Johnson & Chandrasekar, 1992). Differential cooling may be responsible for the ridge/valley and corn-cob textures observed in the matrix material of the tears, but the examinations carried out do not preclude other explanations. As for the network of tubes, differential cooling fails to explain why the tube network exists only just beneath the surface, or why some of the tubes on the underside of the crust are hollow and empty while others contain solid material. A potential mechanism for the network is that the

tubes are the expression of the foamy interior of the tears butting-up against the glassy exterior crust. The interiors of Pele's tears from Kilauea and nearby volcanoes may be particularly foamy due to the high polydispersivity of bubbles in Hawaiian basalts (Colombier et al., 2021). As vesicles contact the crust during expansion, they may flatten out in a disc shape and collide with each other, at which point surface tension forces shape them into a more stable tube configuration. The tubes containing solid fragments of material may be segments of this network which collapsed in on themselves during cooling. Ultimately, from these examinations alone it is unclear if the network of tubes plays a role in

transporting gasses or yet-molten material within the tears during cooling within or beyond the lava fountain. Further, there is no obvious correlation between the morphology of the sub-crustal surface and that of the undersides of the crust.

Basalts from Kilauea typically have about 10–14 wt% iron (Payne & Mau, 1946), so the measured values of iron may be anomalously high due to buildup of iron oxide from the environment on the surfaces of these tears during weathering. Indeed, some of the tears examined are visibly stained orange, probably by iron oxides. The origin or role of a central divot or cavity is not clear, although work by Moune et al. (2007) showed that areas of Pele's tears that were fractured displayed a deeper layer of zonation. The central divots displayed in these radial structures may be the expression of a bubble which became trapped beneath the newly cooled glassy crust of the tear, potentially with a vent leading to the surface. Through this vent the hot material inside the tear would be able to exchange gas with the atmosphere as predicted by Moune et al. (2007). The exchange of cold atmospheric gases would serve as the cooling front necessary to initiate spherulitic growth of silica-rich minerals. Additionally, the cavity is in keeping with the spherulite interpretation, as previous investigations have indicated that spherulites sometimes have a crystal or cavity in their centers (Chrisholm, 1911; Shtukenberg et al., 2012).

It is important to note that these spherulites must have formed in a very short time. After exiting the column of hot gases associated with the erupting lava fountain, the centers of Pele's tears with a radius of 2 millimeters would have fully cooled below their glass transition temperature after only 0.25 s (Porritt et al., 2012). If the radial structures observed beneath the chilled crust in Pele's tears are indeed spherulitic textures caused by crystal growth and chemical zonation as the composition data indicate, they must have formed within this brief cooling time. It is likely the spherulites did not form before exiting the vent and lava fountain during the eruption, since temperatures of lava fountains in the proximity of Kilauea have been observed to range from 1060° to 1190 °C (Ault et al., 1961). Models of spherulite formation in mid-ocean ridge lavas assume the formation of clinopyroxene spherulites begins between 1107° and 950 °C (Gardner et al., 2014). Assuming the upper range of temperatures in the lava fountains is indicative of the temperature of the melt upon exit from the vent, minerals would not begin to form spherulites in Pele's tears until they exited the vent and were higher in the lava fountain.

Our interpretation of the results provided by this study and the work of others lead us to postulate the following timeline of spherulite formation in Pele's tears: as magma made buoyant by the nucleation and growth of exsolved bubbles ascends through the vent, lava fountaining is triggered as the expansion of bubbles leads to fragmentation that converts the magma from a bubbly liquid with a continuous liquid phase to a gassy spray of droplets entrained in continuous gas medium (Housley, 1978; Head & Wilson, 1987; Shimozuru, 1994; Wilson et al., 1995; Jones et al., 2019). Upon exiting the vent, the melt is between 1060° and 1190 °C (Ault et al., 1961). The entrained melt fragments from bubble walls and Plateau borders in the hot gas column of the lava fountain round themselves under surface tension forces as they ascend, subsequently developing a glassy crust upon exiting the fountain and becoming exposed to comparably cold atmospheric air (Porritt et al., 2012; Wygel et al., 2019). This glassy crust, and possibly vesicles that penetrate the

surface, act as a cooling front to initiate spherulite growth. Spherulite growth may begin while the tear is still in the lava fountain, but no spherulites have been observed in the glassy crust of any tears. After 0.25 s of exposure to an ambient air temperature of 25°C, Pele's tears with diameters up to 2 millimeters will have completely cooled to below glass transition temperature (Porritt et al., 2012). Any subsequent generation of spherulites in Pele's tears beyond this point would be through devitrification of the glass, but no distinct evidence has been found for this in the samples observed from Mauna Ulu since the spherulites are found only beneath the surface.

The lack of any spherulites that penetrate the glassy outer crust of the tears likewise indicates spherulite formation does not begin until after the tear exits the lava fountain and its surface has chilled. Further, prior to fragmentation in the lava fountain, the bubble walls and Plateau borders within the erupting magmatic foam would have had a completely different geometry than the spheroids resulting from surface tension-induced relaxation prior to cooling. The potential influence of pre-fragmentation configuration on the position of radial structures and sub-crustal tubes remains unexplored. As such, the process that created the tubes on the underside of the crusts and the textures observed in the matrix of the tears represents a new knowledge gap and will require further targeted experimentation to be described with confidence.

Conclusion

The radial structures observed beneath the glassy surface of Pele's tears from Mauna Ulu are likely the result of chemical zonation occurring within the tear as it cooled, potentially associated with micro-crystallization. This interpretation is consistent with observed element mapping and by linear profile chemical analysis. The textures observed within the matrix of the tears may be caused by tensile stresses imparted within the tears as they cool from the outside in, or by another mechanism entirely. This phenomenon and the network of tubes on the underside of the crust are a puzzle and represent an area for future research and experimentation.

Investigators who wish to close this knowledge gap regarding the nature and origin of the network of subsurface tubes discovered in Pele's tears during this exploratory study may take advantage of synchrotron X-ray sources to create high resolution 3-D models of tears between 30 and 200 μm in diameter with structures in the 1–10 μm range (beyond the resolution of standard X-ray sources). Such models should enable investigators to map the tube network in place and determine how it interacts with both the surfaces above and the deeper interior of the pyroclasts below. In the end, this should lead to a more complete understanding of the eruption dynamics of lava fountains, the lava flows that emerge from them, and the associated volcanic hazards to neighboring communities.

Data availability statement

The original contributions presented in the study are included in the article/supplementary material, further inquiries can be directed to the corresponding author.

Author contributions

SM collected samples, conducted SEM imagery and EDX analysis, manuscript writing, and figure preparation. DS conducted data and imagery interpretation, abstract writing, text, and figure editing.

Acknowledgments

The authors would like to thank Dr. Carolyn Parcheta of the Hawaiian Volcano Observatory for her assistance and guidance during sample collection, Dr. Tamara Carley of Lafayette College for thoughtful advice and suggestions, Fabian Wadsworth for fruitful discussions and insights, and two reviewers for detailed comments and suggestions.

References

- Ault, W. U., Eaton, J. P., and Richter, D. H. (1961). Lava temperatures in the 1959 Kilauea eruption and cooling lake. *GSA Bull.* 72 (5), 791–794. doi:10.1130/0016-7606(1961)72[791:littke]2.0.co;2
- Browning, J., Tuffen, H., James, M., Owen, J., Castro, J., Halliwell, S., et al. (2020). Post-fragmentation vesiculation timescales in hydrous rhyolitic bombs from Chaiten volcano. *J. Afr. Earth Sci.* 104, 102807. doi:10.1016/j.james.2020.102807
- Cannata, C. B., De Rosa, R., Donato, P., Donato, S., Lanzafame, G., Mancini, L., et al. (2019). First 3D imaging characterization of Pele's hair from Kilauea volcano (Hawaii). *Sci. Rep.* 9 (1), 1711. doi:10.1038/s41598-018-37983-9
- H. Chrisholm (Editor) (1911). "Spherulites," *Encyclopedia britannica*. 11 (Cambridge, United Kingdom: Cambridge University Press), Vol. 25, 661.
- Colombier, M., Vasseur, J., Houghton, B. F., Cáceres, F., Scheu, B., Kueppers, U., et al. (2021). Degassing and gas percolation in basaltic magmas. *Earth Planet. Sci. Lett.* 573, 117134. doi:10.1016/j.epsl.2021.117134
- Dietrich, R. V., and Skinner, B. J. (1979). "Glasses," in *Rocks and rock minerals* (New Jersey, United States: John Wiley & Sons, Inc), 151–159.
- Fowler, A. D., Berger, B., Shore, M., Jones, M. I., and Ropchan, J. (2002). Supercooled rocks: Development and significance of varioles, spherulites, dendrites and spinifex in Archaean volcanic rocks, Abitibi Greenstone belt, Canada. *Precambrian Res.* 115 (1–4), 311–328. doi:10.1016/S0301-9268(02)00014-1
- Gardner, J. E., Befus, K. S., Miller, N. R., and Monecke, T. (2014). Cooling rates of mid-ocean ridge lava deduced from clinopyroxene spherulites. *J. Volcanol. Geotherm. Res.* 282, 1–8. doi:10.1016/j.jvolgeores.2014.05.023
- Gerlach, T. M. (1986). Exsolution of H₂O, CO₂, and S during eruptive episodes at kilauea volcano, Hawaii. *J. Geophys. Res. Solid Earth* 91 (B12), 12177–12185. doi:10.1029/JB091iB12p12177
- Head, J. W., III, and Wilson, L. (1987). Lava fountain heights at Pu'u O'o, Kilauea, Hawaii: Indicators of amount and variations of exsolved magma volatiles. *J. Geophys. Res. Solid Earth* 92 (B13), 13715–13719. doi:10.1029/JB092iB13p13715
- Housley, R. M. (1978). "Modeling lunar volcanic eruptions," Lunar and planetary science conference, 2, 1473–1484. Available at: <https://adsabs.harvard.edu/full/1978LPSC.9.1473H>.
- Johnson, W., and Chandrasekar, S. (1992). Volcanic bombs—their form and physical structure: Comparison with cast iron cannon balls. *Int. J. Impact Eng.* 12 (3), 459–467. doi:10.1016/0734-743X(92)90189-Z
- Jones, T. J., Reynolds, C. D., and Boothroyd, S. C. (2019). Fluid dynamic induced break-up during volcanic eruptions. *Nat. Commun.* 10 (1), 3828. doi:10.1038/s41467-019-11750-4
- Kirkpatrick, R. J., Klein, L., Uhlmann, D. R., and Hays, J. F. (1979). Rates and processes of crystal growth in the system anorthite-albite. *J. Geophys. Res. Solid Earth* 84 (B7), 3671–3676. doi:10.1029/JB084iB07p03671
- Lofgren, G. (1971b). Experimentally produced devitrification textures in natural rhyolitic glass. *GSA Bull.* 82 (1), 111–124. doi:10.1130/0016-7606(1971)82[111:epdntn]2.0.co;2
- Lofgren, G. (1971a). Spherulitic textures in glassy and crystalline rocks. *J. Geophys. Res.* 76 (23), 5635–5648. doi:10.1029/JB076i023p05635
- Monecke, T., Renno, A. D., and Herzig, P. M. (2003). Primary clinopyroxene spherulites in basaltic lavas from the Pacific-Antarctic Ridge. *J. Volcanol. Geotherm. Res.* 130, 51–59. doi:10.1016/S0377-0273(03)00278-6

Conflict of interest

The authors declare that the research was conducted in the absence of any commercial or financial relationships that could be construed as a potential conflict of interest.

Publisher's note

All claims expressed in this article are solely those of the authors and do not necessarily represent those of their affiliated organizations, or those of the publisher, the editors and the reviewers. Any product that may be evaluated in this article, or claim that may be made by its manufacturer, is not guaranteed or endorsed by the publisher.

Moone, S., Faure, F., Gauthier, P.-J., and Sims, K. W. W. (2007). Pele's hairs and tears: Natural probe of volcanic plume. *J. Volcanol. Geotherm. Res.* 164, 244–253. doi:10.1016/j.jvolgeores.2007.05.007

Namiki, A., Patrick, M. R., Manga, M., and Houghton, B. F. (2021). Brittle fragmentation by rapid gas separation in a Hawaiian fountain. *Nat. Geosci.* 14, 242–247. doi:10.1038/s41561-021-00709-0

Parcheta, C. E., Houghton, B. F., and Swanson, D. A. (2013). Contrasting patterns of vesiculation in low, intermediate, and high Hawaiian fountains; a case study of the 1969 Mauna Ulu eruption. *J. Volcanol. Geotherm. Res.* 225, 79–89. doi:10.1016/j.jvolgeores.2013.01.016

Parcheta, C. E., Houghton, B. F., and Swanson, D. A. (2012). Hawaiian fissure fountains 1: Decoding deposits—episode 1 of the 1969–1974 Mauna Ulu eruption. *Bull. Volcanol.* 74, 1729–1743. doi:10.1007/s00445-012-0621-1

Payne, J. H., and Mau, K. T. (1946). A study of the chemical alteration of basalt in the kilauea region of Hawaii. *J. Geol.* 54 (6), 345–358. doi:10.1086/625375

Phillips, W. J. (1973). Interpretation of crystalline spheroidal structures in igneous rocks. *Lithos* 6 (3), 235–244. doi:10.1016/0024-4937(73)90084-4

Porritt, L. A., Russell, J. K., and Quane, S. L. (2012). Pele's tears and spheres: Examples from kilauea iki. *Earth Planet. Sci. Lett.* 333–334, 171–180. doi:10.1016/j.epsl.2012.03.031

Proussevitch, A. A., and Sahagian, D. L. (1996). Dynamics of coupled diffusive and decompressive bubble growth in magmatic systems. *J. Geophys. Res. Solid Earth* 101 (B8), 17447–17455. doi:10.1029/96JB01342

Quane, S., and Andrews, B. (2020). Breadcrust bubbles: Ash particles recording post-fragmentation brittle-ductile deformation. *Geology* 48, 1205–1209. doi:10.1130/G47811.1

Shimozuru, D. (1994). Physical parameters governing the formation of Pele's hair and tears. *Bull. Volcanol.* 56, 217–219. doi:10.1007/bf00279606

Shtukenberg, A. G., Punin, Y. O., Gunn, E., and Kahr, B. (2012). Spherulites. *Chem. Rev.* 112 (3), 1805–1838. doi:10.1021/cr200297f

Smith, R. K., Tremallo, R. L., and Lofgren, G. E. (2001). Growth of megaspherulites in a rhyolitic vitrophyre. *Am. Mineralogist* 86 (5–6), 589–600. doi:10.2138/am-2001-5-601

Swanson, D. A., Duffield, D. A., Jackson, D. B., and Peterson, D. W. (1979). *Chronological narrative of the 1969–71 Mauna Ulu eruption of kilauea volcano, Hawaii*. Volcano, Hawaii: USGS. U.S. Geological Survey Professional Paper 1056.

Thivet, S., Gurioli, L., Di Muro, A., Eychenne, J., Besson, P., and Nedelec, J. M. (2020). Variability of ash deposits at piton de la Fournaise (La reunion island): Insights into fragmentation processes at basaltic shield volcanoes. *Bull. Volcanol.* 82, 63–20. doi:10.1007/s00445-020-01398-0

Tuffen, H., Farquharson, J., Wadsworth, F., Webb, C., Owen, J., Castro, J., et al. (2022). Mid-loaf crisis: Internal breadcrust surfaces in rhyolitic pyroclasts reveal dehydration quenching. *Geology* 50, 1058–1062. doi:10.1130/G49959.1

Wilson, L., Parfitt, E. A., and Head, J. W., III. (1995). Explosive volcanic eruptions—VIII. The role of magma recycling in controlling the behaviour of Hawaiian-style lava fountains. *Geophys. J. Int.* 121 (1), 215–225. doi:10.1111/j.1365-246X.1995.tb03522.x

Wygel, C. M., Peters, S. C., McDermott, J. M., and Sahagian, D. L. (2019). Bubbles and dust: Experimental results of dissolution rates of metal salts and glasses from volcanic ash deposits in terms of surface area, chemistry, and human health impacts. *Geohealth* 3, 338–355. doi:10.1029/2018GH000181